PNAS
www.pnas.org

Supplementary Information for

Pleiotropic neuroprotective effects of taxifolin in cerebral amyloid angiopathy

Takayuki Inoue, Satoshi Saito, Masashi Tanaka, Hajime Yamakage, Toru Kusakabe, Akira Shimatsu, Masafumi Ihara, and Noriko Satoh-Asahara

Corresponding author:
Masashi Tanaka
Email: masashi.7.tanaka@gmail.com

This PDF file includes:

Figs. S1 to S7
Tables S1 to S2
References for SI reference citations

www.pnas.org/cgi/doi/10.1073/pnas.1901659116

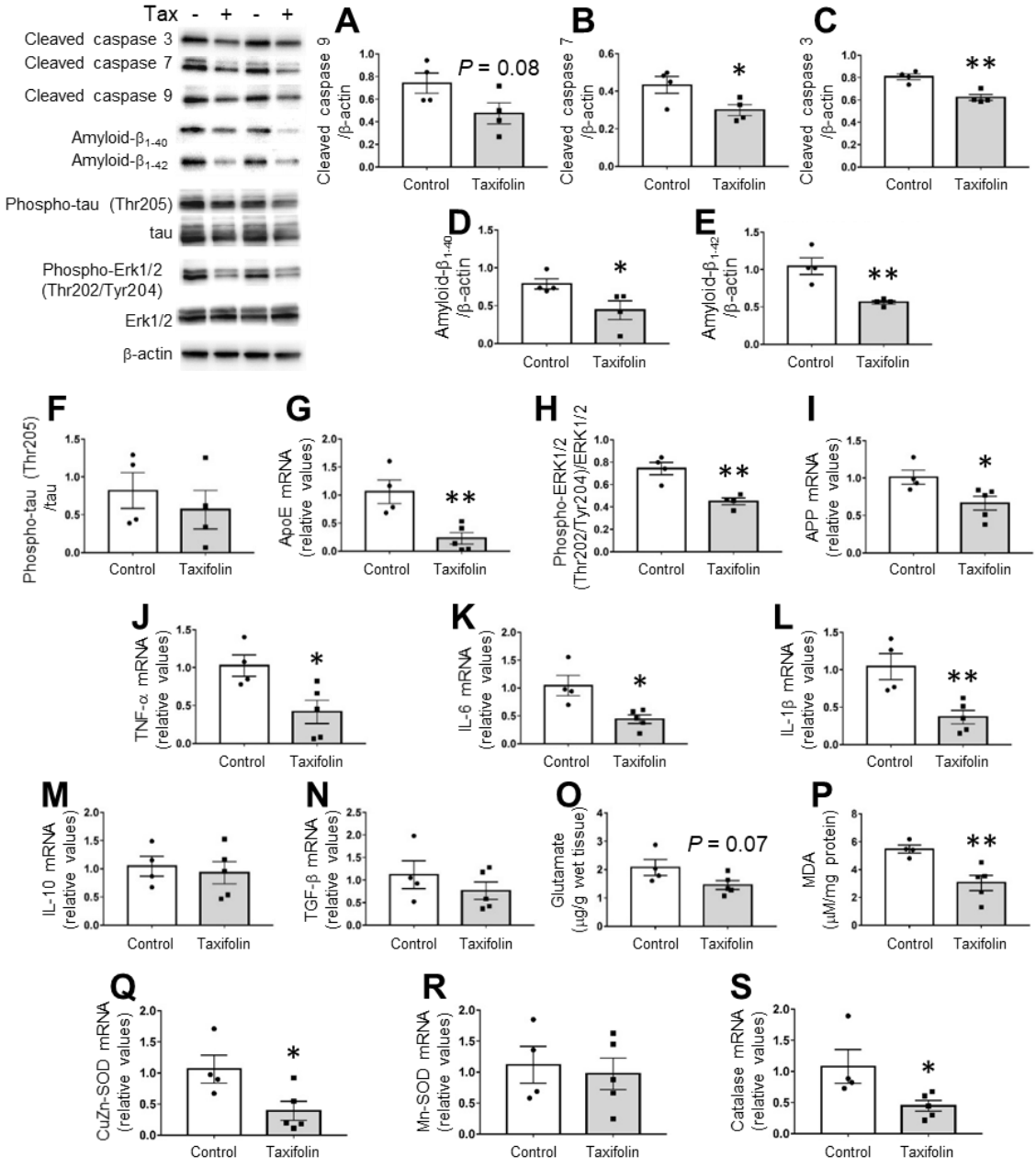

Figure S1. Protective effects of taxifolin on brain cells in the cortex of Tg-SwDI mice. The histograms compare values for cortical tissue for the same 14-month-old Tg-SwDI mice that received either the control diet (n = 4) or taxifolin-containing chow (n = 5) for 13 months. Relative amounts were analyzed by western blot and densitometry, and mRNA expression levels obtained by quantitative RT-PCR and normalized to that of

GAPDH. The upper left image shows representative immunoblots. (*A*–*C*) Activation levels of apoptosis-related caspases cleaved caspase-9 (*A*), cleaved caspase-7 (*B*), and cleaved caspase-3 (*C*) relative to β-actin. (*D*–*F*) Accumulation levels of amyloid-β and hyperphosphorylated tau proteins in the cortical tissue: amyloid-$\beta_{1\text{-}40}$ (*D*) and amyloid-$\beta_{1\text{-}42}$ (*E*) relative to β-actin and phospho-tau (Thr205) relative to total tau (*F*). (*G*–*I*) Activation levels of pathways involved in amyloid-β production in the cortical tissue: mRNA levels of ApoE (*G*) and APP (*I*), and the amount of phospho-ERK1/2 (Thr202/Tyr204) relative to total ERK (*H*). (*J*–*N*) mRNA expression levels of proinflammatory and anti-inflammatory cytokines TNF-α (*J*), IL-6 (*K*), IL-1β (*L*), IL-10 (*M*), and TGF-β (*N*). (*O*) Glutamate levels in the cortical tissue. (*P*) Levels of free lipid peroxides, malondialdehyde (MDA), in the cortical tissue. (*Q*–*S*) mRNA expression levels of the oxidative stress-responsive genes CuZn-SOD (*Q*) and Mn-SOD (*R*), and of catalase (*S*). Data are expressed as mean ± SEM (control, n = 4; taxifolin, n = 5). *P* values were determined by Student's *t*-test. **P* < 0.05; ***P* < 0.01.

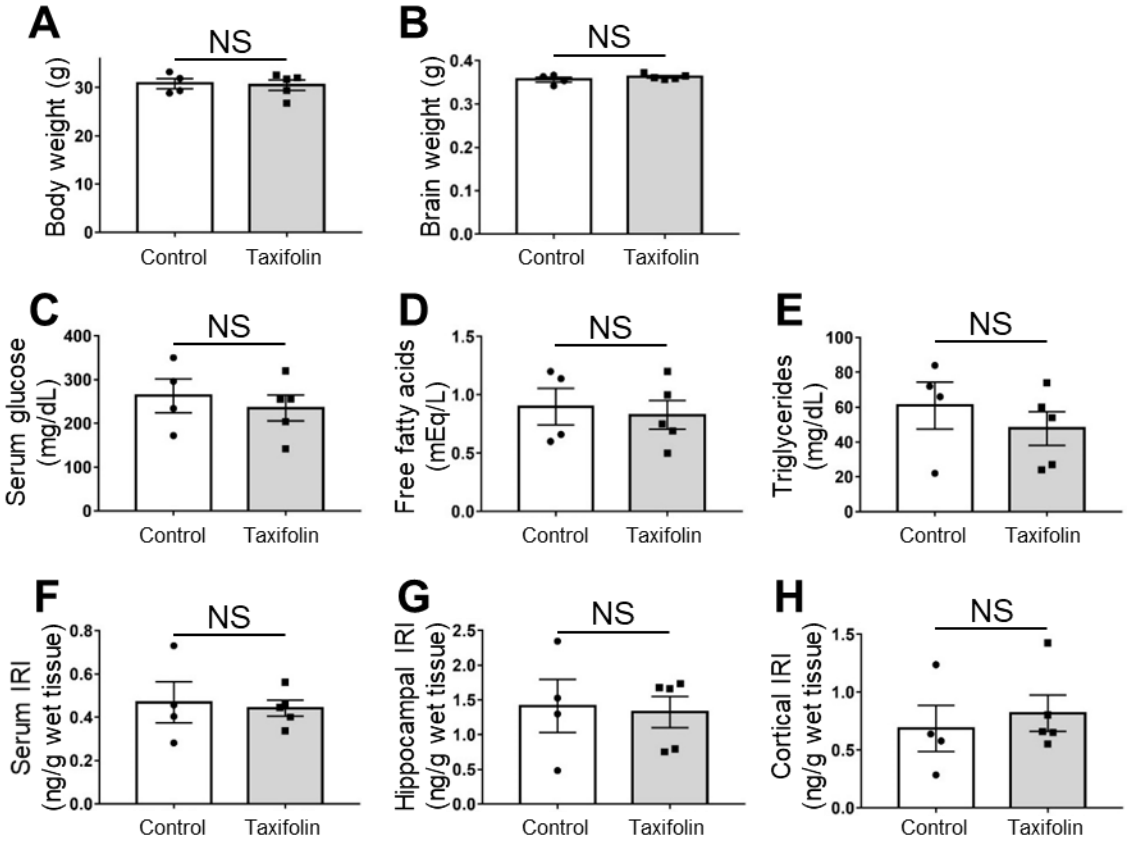

Figure S2. Effects of taxifolin on the anthropometric and metabolic parameters of Tg-SwDI mice. Results for 14-month-old Tg-SwDI mice that received either the control diet (n = 4) or a diet containing taxifolin (n = 5) for 13 months. (*A* and *B*) Weights of the body (*A*) and brain (*B*). (*C–E*) Serum levels of glucose (*C*), free fatty acids (*D*), and triglycerides (*E*). (*F–H*) Serum (*F*), hippocampal (*G*), and cortical (*H*) insulin levels. Hippocampal and cortical tissues were separately homogenized, centrifuged, and the supernatant was used to analyze insulin level. The levels of insulin in the serum, hippocampal tissue, and cortical tissue were measured by ELISA. IRI, immunoreactive insulin. Data are expressed as mean ± SEM (control, n = 4; taxifolin, n = 5). Statistical significance was examined by Student's *t*-test. NS, not significant.

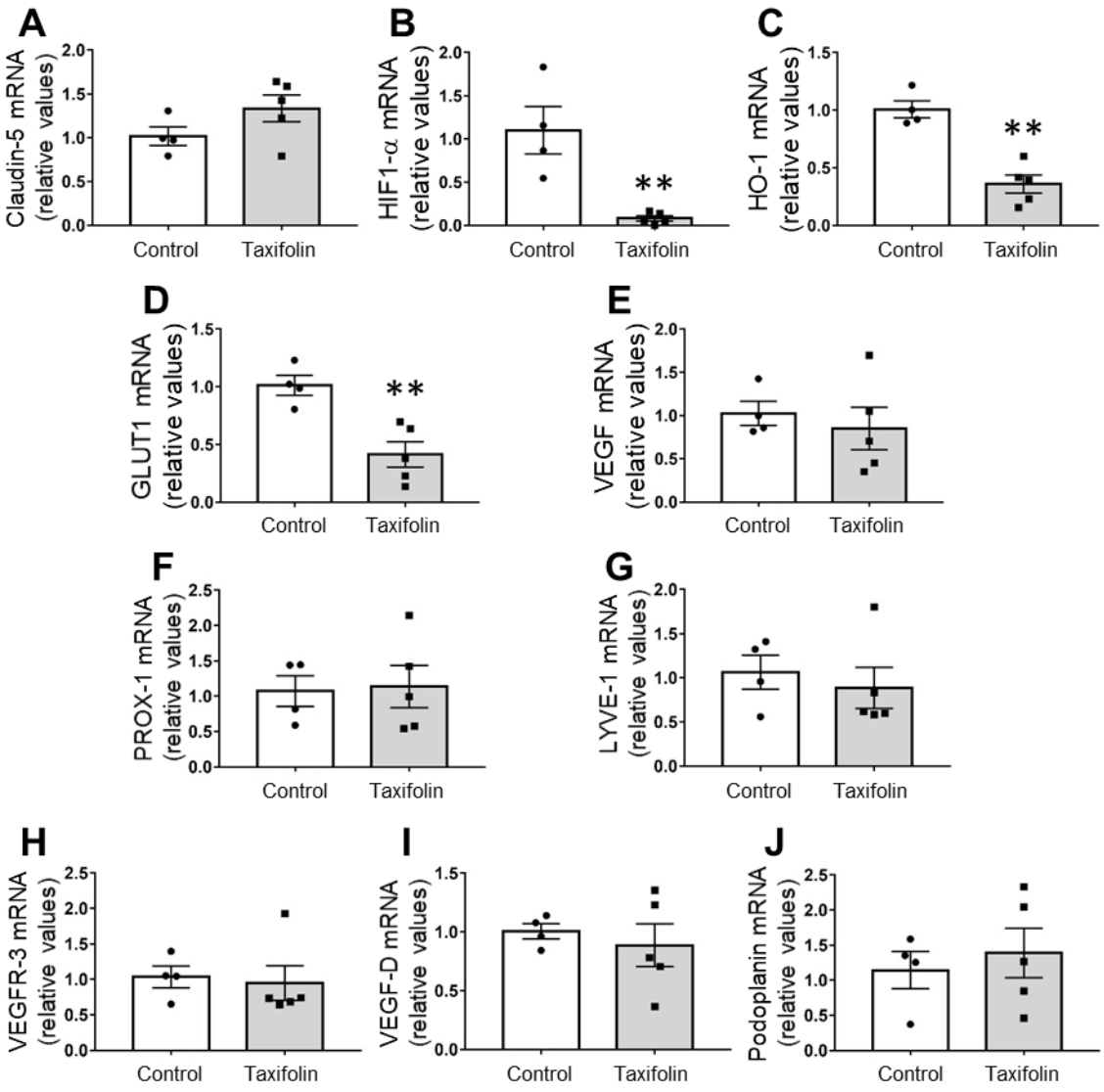

Figure S3. Effects of taxifolin on expression levels of blood and lymphatic vasculature-related or hypoxia-responsive genes in the cortex of Tg-SwDI mice. Results for the cortical tissue from 14-month-old Tg-SwDI mice that received either the control diet (n = 4) or a diet containing taxifolin (n = 5) for 13 months. mRNA levels were measured by quantitative RT-PCR and normalized to GAPDH. (*A*) mRNA expression level of the tight-junction-related cerebrovascular endothelial marker claudin-5. (*B–E*) mRNA expression levels of hypoxia-responsive genes in the cortical tissue: HIF-1α (*B*), HO-1 (*C*), GLUT1 (*D*), and VEGF (*E*). (*F–J*) Gene expression levels of markers for lymphatic

endothelial cells: PROX-1 (*F*), LYVE-1 (*G*), VEGFR-3 (*H*), VEGF-D (*I*), and podoplanin (*J*). Data are expressed as mean ± SEM (control, n = 4; taxifolin, n = 5). *P* values were determined by Student's *t*-test. $^{**}P < 0.01$.

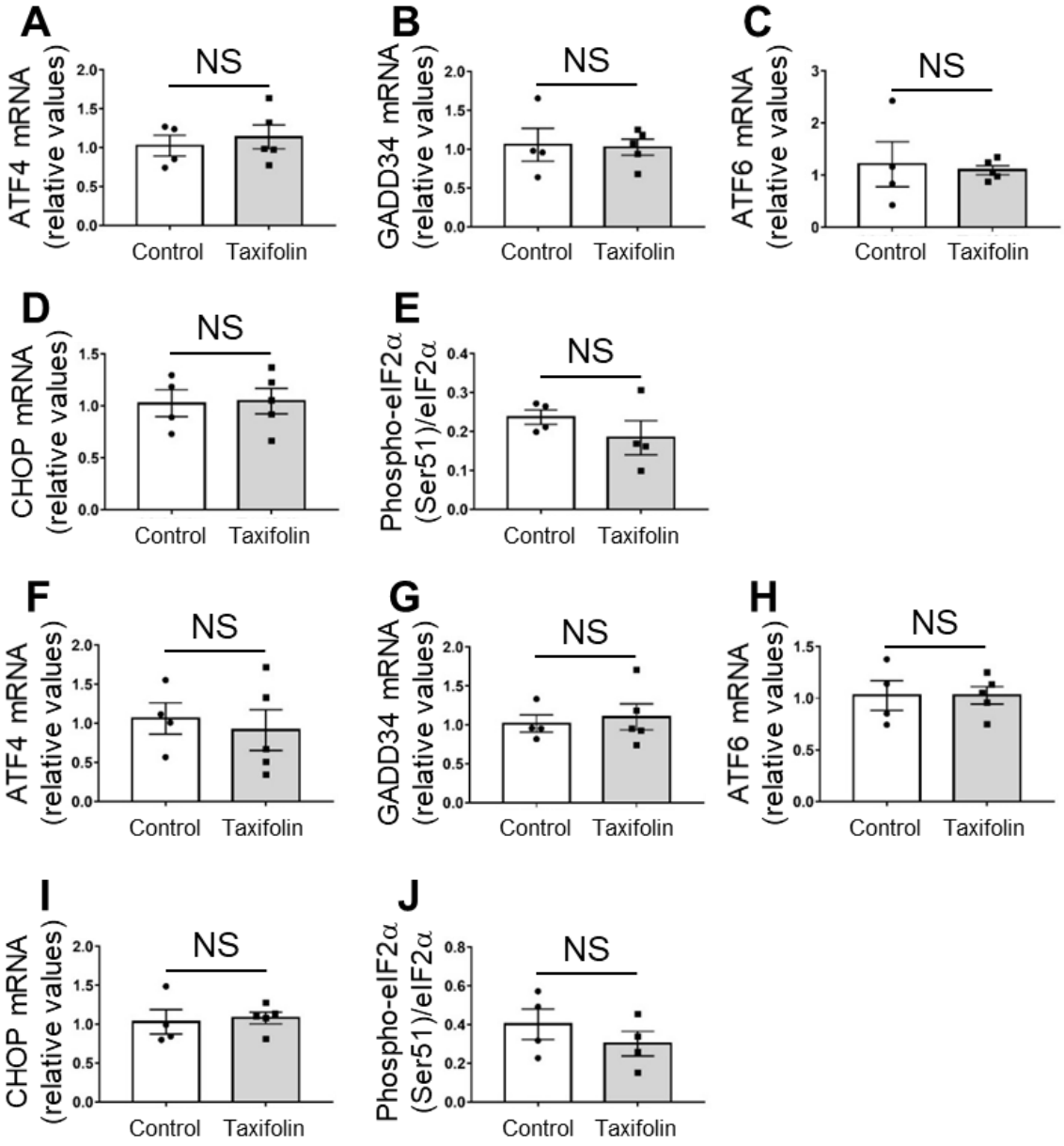

Figure S4. Effects of taxifolin on endoplasmic reticulum (ER) stress markers in the hippocampus and cortex of Tg-SwDI mice. Results for hippocampal and cortical tissue from 14-month-old Tg-SwDI mice that received either the control diet (n = 4) or a diet containing taxifolin (n = 5) for 13 months. mRNA levels were measured by quantitative RT-PCR and normalized to GAPDH. Relative amounts were obtained by western blot and densitometry. (*A–E*) mRNA expression levels of ER stress markers in the

hippocampus: ATF4 (*A*), GADD34 (*B*), ATF6 (*C*), and CHOP (*D*), and the amount of phospho-eIF2α (Ser51) relative to total eIF2α (*E*). (*F–J*) mRNA expression levels of ER stress markers in the cortex: ATF4 (*F*), GADD34 (*G*), ATF6 (*H*), and CHOP (*I*), and the amount of phospho-eIF2α (Ser51) relative to total eIF2α (*J*). Data are expressed as mean ± SEM (control, n = 4; taxifolin, n = 5). Statistical significance was determined by Student's *t*-test. NS, not significant.

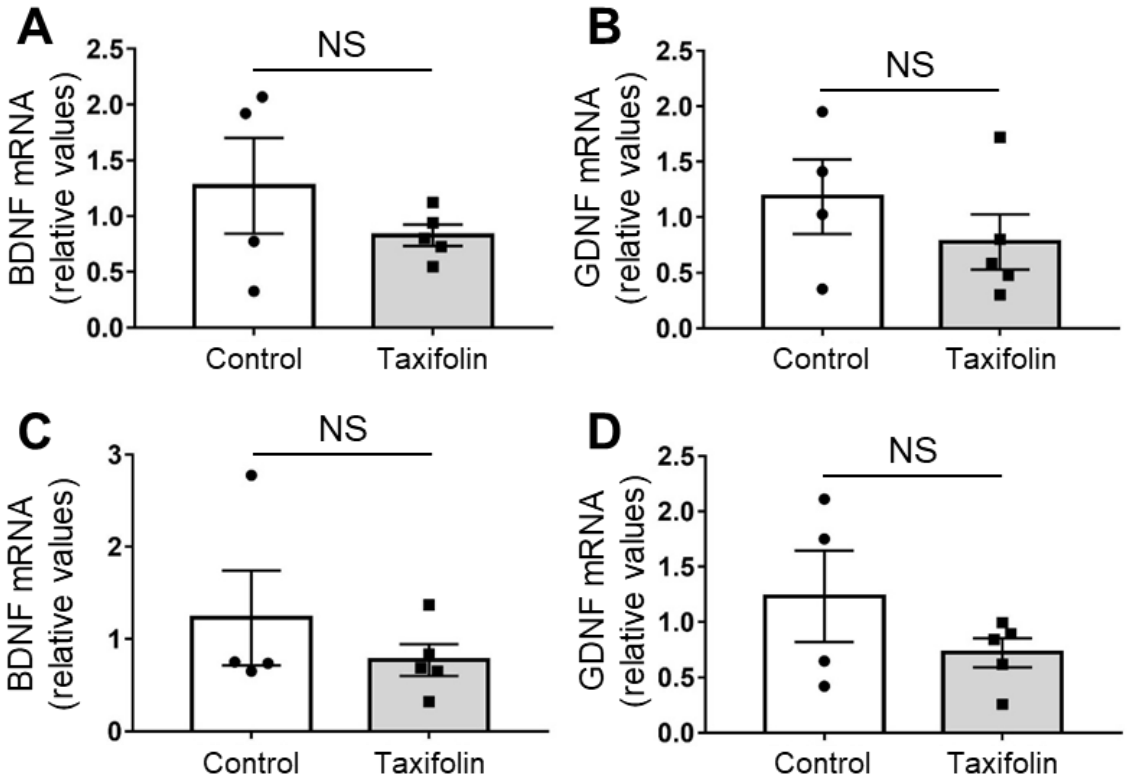

Figure S5. Effects of taxifolin on expression levels of neurotrophic growth factors in the hippocampus and cortex of Tg-SwDI mice. Results for 14-month-old Tg-SwDI mice that received either the control diet (n = 4) or a diet containing taxifolin (n = 5) for 13 months. mRNA levels were measured by quantitative RT-PCR and normalized to GAPDH. (*A–D*) mRNA expression levels of neurotrophic growth factors in the hippocampus (*A* and *B*) and cortex (*C* and *D*): BDNF (*A* and *C*) and GDNF (*B* and *D*). Data are expressed as mean ± SEM (control, n = 4; taxifolin, n = 5). Statistical significance was examined by Student's *t*-test. NS, not significant.

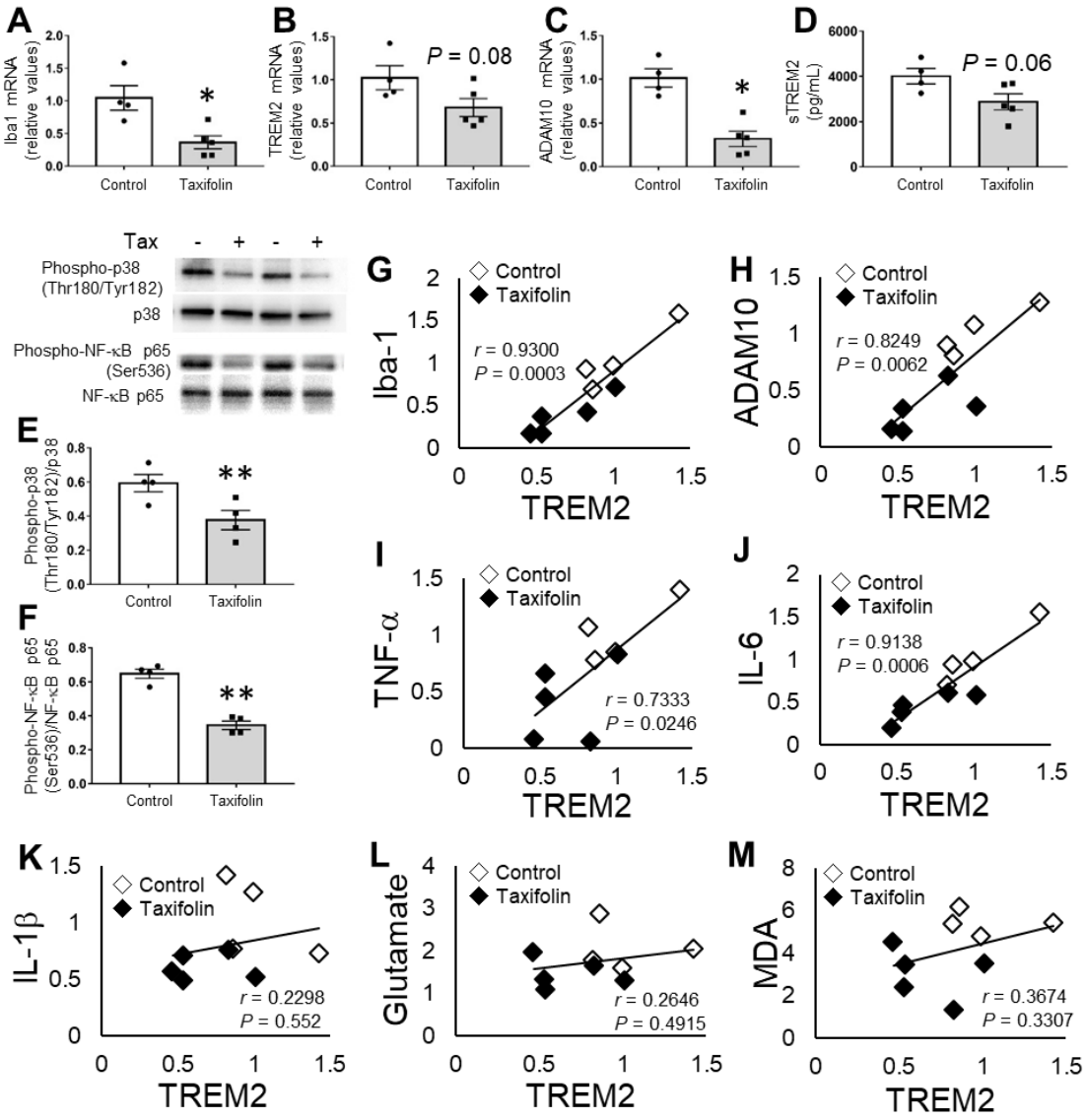

Figure S6. Beneficial effects of taxifolin on proinflammatory phenotypes of microglia in the cortex of Tg-SwDI mice. Results for the cortical tissue from 14-month-old Tg-SwDI mice that received either the control diet (n = 4) or a diet containing taxifolin (n = 5) for 13 months. mRNA levels were measured by quantitative RT-PCR and normalized to GAPDH. Relative amounts were obtained by western blot and densitometry. Representative images are shown to the upper left. (*A–C*) mRNA expression levels of Iba-1 (*A*), TREM2 (*B*), and ADAM10 (*C*). (*D*) Concentration of sTREM2 in the cortical tissue. (*E* and *F*) Activation levels of proinflammatory signaling pathways in the cortical

tissue: amounts of phospho-p38 (Thr180/Tyr182) relative to total p38 (*E*) and phospho-NF-κB p65 (Ser536) relative to total NF-κB p65 (*F*). (*G–M*) Associations between expression levels of TREM2 and levels of Iba-1 (*G*), ADAM10 (*H*), TNF-α (*I*), IL-6 (*J*), IL-1β (*K*), glutamate (*L*), and lipid peroxidation (*M*) in the cortical tissue. *A–F*, Data are expressed as mean ± SEM (control, n = 4; taxifolin, n = 5); *P* values were determined by Student's *t*-test; **P* < 0.05; ***P* < 0.01. *G–M*, Pearson's correlation coefficients (*r*) were used to test the associations of interest.

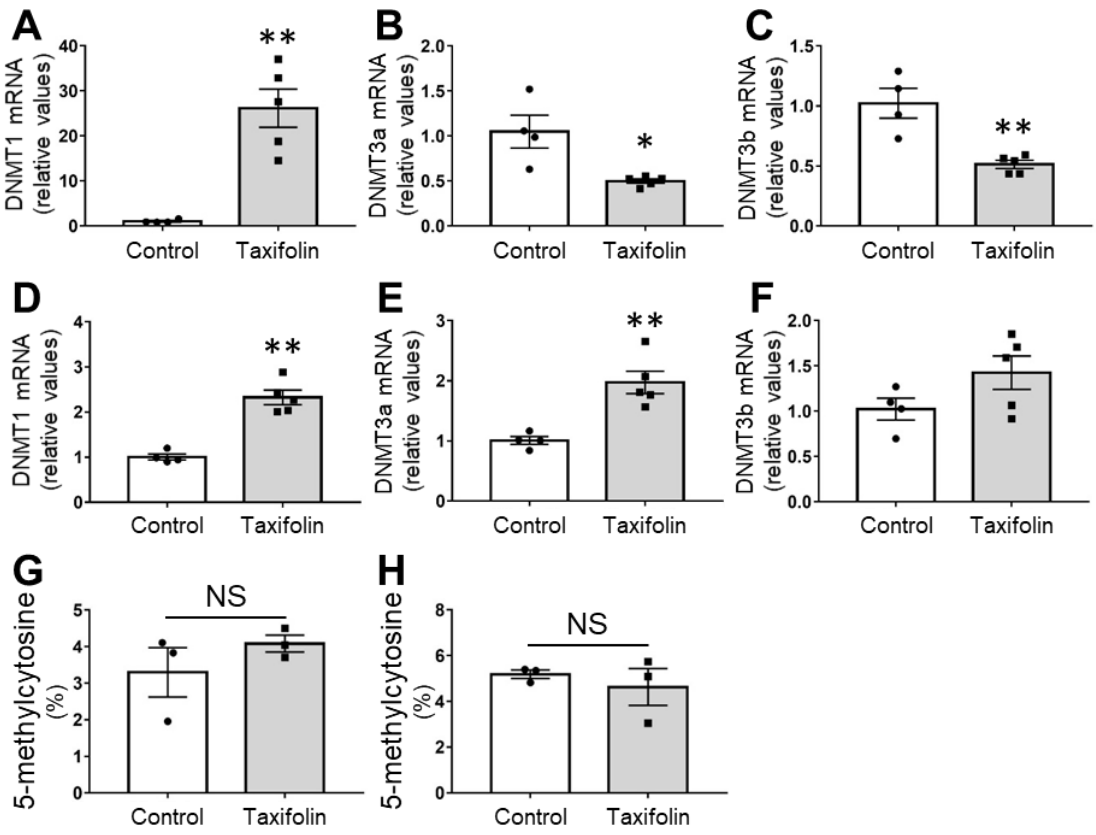

Figure S7. Effects of taxifolin on the expression levels of DNA methyltransferases and the global DNA methylation levels in genomic DNA in the hippocampus and cortex of Tg-SwDI mice. Results for hippocampal and cortical tissue from 14-month-old Tg-SwDI mice that received either the control diet (n = 4) or a diet containing taxifolin (n = 5) for 13 months. mRNA levels were measured by quantitative RT-PCR and normalized to GAPDH. (*A–F*) mRNA expression levels of DNMT1 (*A* and *D*), DNMT3a (*B* and *E*), and DNMT3b (*C* and *F*) in the hippocampal (*A–C*) and cortical tissue (*D–F*). (*G* and *H*) Global 5-methylcytosine levels in genomic DNA in the hippocampal (*G*) and cortical (*H*) tissue. Genomic DNA was separately purified from the hippocampal or cortical tissue and the 5-methylcytosine fraction of DNA was detected using capture and detection antibodies, followed by colorimetric quantification. The 5-methylcytosine contents are shown as a percentage of total DNA. Statistical significance was examined by Student's *t*-test. **P* < 0.05; ***P* < 0.01; NS, not significant.

Table S1. List of antibodies used in western blot and immunohistochemistry.

Antibodies	Suppliers	Dilution	Isotype
Phospho-p44/42 MAPK (Erk1/2) (Thr202/Tyr204)	Cell Signaling Technology	1:1000	Rabbit mAb
p44/42 MAPK (Erk1/2) (137F5)	Cell Signaling Technology	1:1000	Rabbit mAb
β-Amyloid (1-40 Specific) (D8Q7I)	Cell Signaling Technology	1:1000	Rabbit mAb
β-Amyloid (1-42 Specific) (D9A3A)	Cell Signaling Technology	1:1000	Rabbit mAb
Phospho-Tau (Thr205)	Abcam	1:1000	Rabbit pAb
Tau antibody [TAU-5]	Abcam	1:500	Mouse mAb
Phospho-p38 MAPK (Thr180/Tyr182)	Cell Signaling Technology	1:1000	Rabbit mAb
p38 MAPK	Cell Signaling Technology	1:1000	Rabbit mAb
Phospho-NF-κB p65 (Ser536)	Cell Signaling Technology	1:1000	Rabbit mAb
NF-κB p65（C22B4)	Cell Signaling Technology	1:1000	Rabbit mAb
Phospho-eIF2α (Ser51)	Cell Signaling Technology	1:1000	Rabbit mAb
eIF2α	Cell Signaling Technology	1:1000	Rabbit mAb
Cleaved Caspase-3 (Asp175) (5A1E)	Cell Signaling Technology	1:1000	Rabbit mAb
Cleaved Caspase-7 (Asp198) (D6H1)	Cell Signaling Technology	1:1000	Rabbit mAb
Cleaved Caspase-9 (Asp330) (D2D4)	Cell Signaling Technology	1:1000	Rabbit mAb
β-actin	Cell Signaling Technology	1:1000	Rabbit mAb
Iba-1*	Abcam	1:500	Goat pAb
TNF-α*	Abcam	1:100	Rabbit pAb
TREM2*	Bios antibodies	1:250	Rabbit pAb

*Antibodies for immunohistochemistry.

Table S2. List of primer sequences.

Target gene	Forward primer (5'-3')	Reverse primer (5'-3')	Reference
ADAM10	GTGCCAGTACAGGCTCTTTGC	CACAGTAGCCTCTGAAGTCATTACATG	1
ApoE	CTGACAGGATGCCTAGCCG	CGCAGGTAATCCCAGAAGC	2
APP	TGCAGCAGAACGGATATGAGAAT	GTCAAAAGCCGAGGGTGAGTAAA	3
ATF4	CTATGGATGATGGCTTGGCC	CCGGAAAAGGCATCCTCC	4
ATF6	TGGGAGTGAGCTGCAAGTGT	ATAAGGGGGAACCGAGGAG	4
BDNF	GGTATCCAAAGGCCAACTGA	CTTATGAATCGCCAGCCAAT	5
Catalase	GCAGATACCTGTGAACTGTC	GTAGAATGTCCGCACCTGAG	6
CHOP	CCACCACACCTGAAAGCAGAA	AGGTGAAAGGCAGGGACTCA	This study
Claudin-5	CAGTTAAGGCACGGGTAGCA	GGCACCGTCGGATCATAGAA	7
CuZn-SOD	AAGGCCGTGTGCGTGCTGAA	CAGGTCTCCAACATGCCTCT	6
DNMT1	AAGAATGTGTTGTCTACCGAC	CATCCAGGTTGCTCCCCT TG	8
DNMT3a	GAGGGAACTGAGACCCCA C	CTGGAAGGTGAGTCTTGGCA	8
DNMT3b	AGCGGGTATGAGGAGTGCAT	GGGAGCATCCTTCGTGTCTG	8
GADD34	TTACCAGAGACAGGGGTAGGT	GAGGGACGCCCACAACTTC	This study
GDNF	ACCCGCTTCCATAAGGCTTTA	CAGCCTTGTGCCGAAAGAC	5
GLUT-1	CCAGCTGGGAATCGTCGTT	CAAGTCTGCATTGCCCATGAT	9
HIF-1α	CCTTCATCGGAAACTCCAAA	TGGGGCATGGTAAAAGAAAG	10
HO-1	TGAAGGAGGCCACCAAGGAGG	AGAGGTCACCCAGGTAGCGGG	11
Iba-1	GTCCTTGAAGCGAATGCTGG	CATTCTCAAGATGGCAGATC	12
IL-10	CCTGGTAGAAGTGATGCCCC	GAAATCGATGACAGCGCCTC	13
IL-1β	CACAGCAGCACATCAACAAG	GTGCTCATGTCCTCATCCTG	This study
IL-6	AGACAAAGCCAGAGTCCTTCA	GGTCCTTAGCCACTCCTTCTG	13
LYVE-1	CAGCACACTAGCCTGGTGTTA	CGCCCATGATTCTGCATGTAGA	14
Mn-SOD	GCACATTAACGCGCAGATCA	AGCCTCCAGCAACTCTCCTT	6
Podoplanin	CACCTCAGCAACCTCAGAC	ACAGGGCAAGTTGGAAGC	15
Prox-1	GTTCCACAGACCAGACGGAAG	CAGAGGCAGATTGCTCGGAT	16
TGF-β	ACCGCAACAACGCCATCTAT	GTATCAGTGGGGGTCAGCAG	17
TNF-α	GCCTCTTCTCATTCCTGCTTG	CTGATGAGAGGGAGGCCATT	18
TREM2	TGGGACCTCTCCACCAGTT	GTGGTGTTGAGGGCTTGG	19
VEGF	CCACGTCAGAGAGCAACATCA	TCATTCTCTCTATGTGCTGGCTTT	9
VEGF-D	GCTCAAAAGTCTTGCCAGTATGG	AGTTGCCGCAAATCTGGTG	16
VEGFR-3	TGGTACCGGCTCAACCTCTC	CACGTTTTTGCAGTCCAGCA	16
GAPDH	TCCACTCACGGCAAATTCAACG	TAGACTCCACGACATACTCAGC	This study

References

1. Gordon GM, et al. (2011) Comprehensive gene expression profiling and functional analysis of matrix metalloproteinases and TIMPs, and identification of ADAM-10 gene

expression, in a corneal model of epithelial resurfacing. *J Cell Physiol* 226:1461–1470.
2. Tweedie D, et al. (2013) Exendin-4, a glucagon-like peptide-1 receptor agonist prevents mTBI-induced changes in hippocampus gene expression and memory deficits in mice. *Exp Neurol* 239:170–182.
3. Deng M, et al. (2016) beta-asarone improves learning and memory and reduces Acetyl Cholinesterase and Beta-amyloid 42 levels in APP/PS1 transgenic mice by regulating Beclin-1-dependent autophagy. *Brain Res* 1652:188–194.
4. Iwasaki Y, et al. (2014) Activating transcription factor 4 links metabolic stress to interleukin-6 expression in macrophages. *Diabetes* 63:152–161.
5. Akazawa Y, et al. (2013) Forced mastication increases survival of adult neural stem cells in the hippocampal dentate gyrus. *Int J Mol Med* 31:307–314.
6. Jarukamjorn K, Jearapong N, Pimson C, Chatuphonprasert W (2016) A High-Fat, High-Fructose Diet Induces Antioxidant Imbalance and Increases the Risk and Progression of Nonalcoholic Fatty Liver Disease in Mice. *Scientifica (Cairo.)* 2016:5029414.
7. Wang J, et al. (2016) Effects of colistin on amino acid neurotransmitters and blood-brain barrier in the mouse brain. *Neurotoxicol Teratol* 55:32–37.
8. Kozuka C, et al. (2017) Impact of brown rice-specific gamma-oryzanol on epigenetic modulation of dopamine D2 receptors in brain striatum in high-fat-diet-induced obesity in mice. *Diabetologia* 60:1502–1511.
9. Kind KL, Collett RA, Harvey AJ, Thompson JG (2005) Oxygen-regulated expression of GLUT-1, GLUT-3, and VEGF in the mouse blastocyst. *Mol Reprod Dev* 70:37–44.
10. Kupershmidt L, et al. (2011) Novel molecular targets of the neuroprotective/neurorescue multimodal iron chelating drug M30 in the mouse brain. *Neuroscience* 189:345–358.
11. Jeong YH, Oh YC, Cho WK, Lee B, Ma JY (2016) Anti-Inflammatory Effects of Melandrii Herba Ethanol Extract via Inhibition of NF-kappaB and MAPK Signaling Pathways and Induction of HO-1 in RAW 264.7 Cells and Mouse Primary Macrophages. *Molecules* 21.
12. Sandhir R, Onyszchuk G, Berman NE (2008) Exacerbated glial response in the aged mouse hippocampus following controlled cortical impact injury. *Exp Neurol* 213:372–380.
13. Inoue T, et al. (2017) Omega-3 polyunsaturated fatty acids suppress the inflammatory responses of lipopolysaccharide-stimulated mouse microglia by activating SIRT1 pathways. *Biochim Biophys Acta Mol Cell Biol Lipids* 1862:552–560.
14. Flister MJ, Volk LD, Ran S (2011) Characterization of Prox1 and VEGFR-3 expression and lymphatic phenotype in normal organs of mice lacking p50 subunit of NF-kappaB. *Microcirculation* 18:85–101.
15. Kaji C, Tomooka M, Kato Y, Kojima H, Sawa Y (2012) The expression of podoplanin and classic cadherins in the mouse brain. *J Anat* 220:435–446.
16. Nilsson I, et al. (2004) Vascular endothelial growth factor receptor-3 in hypoxia-induced vascular development. *FASEB J* 18:1507–1515.
17. Lyons RE, et al. (2001) Immunological studies of chronic ocular toxoplasmosis: up-regulation of major histocompatibility complex class I and transforming growth factor beta and a protective role for interleukin-6. *Infect Immun* 69:2589–2595.
18. Yamakawa I, et al. (2011) Inactivation of TNF-α ameliorates diabetic neuropathy in mice. *Am J Physiol Endocrinol Metab* 301:E844–E852.
19. Parodi B, et al. (2015) Fumarates modulate microglia activation through a novel HCAR2 signaling pathway and rescue synaptic dysregulation in inflamed CNS. *Acta Neuropathol* 130:279–295.